

Constraining slope parameter of symmetry energy from nuclear structure

T. Inakura^{1,2,3} and H. Nakada¹

¹*Department of Physics, Graduate School of Science, Chiba University, Chiba 263-8522, Japan*

²*Yukawa Institute of Theoretical Physics, Kyoto University, Kyoto 606-8502, Japan*

³*Department of Physics, Niigata University, Niigata 950-2181, Japan*

Four quantities deducible from nuclear structure experiments have been claimed to correlate to the slope parameter L of the symmetry energy; the neutron skin thickness, the cross section of low-energy dipole (LED) mode, dipole polarizability α_D , and $\alpha_D S_0$ (i.e. product of α_D and the symmetry energy S_0). By the calculations in the Hartree-Fock plus random-phase approximation with various effective interactions, we compare the correlations between L and these four quantities. The correlation derived from different interactions and the correlation from a class of interactions that are identical in the symmetric matter as well as in S_0 are simultaneously examined. These two types of correlations may behave differently, as exemplified in the correlation of α_D to L . It is found that the neutron skin thickness and $\alpha_D S_0$ correlate well to L , and therefore are suitable for narrowing down the value of L via experiments. The LED emergence and upgrowth makes the $\alpha_D S_0$ - L correlation strong, although these correlations are disarranged when neutron halo appears in the ground state.

PACS numbers: 21.65.-f, 21.65.Mn, 24.30.Cz, 24.30.Gd, 21.60.Jz, 25.20.-x

I. INTRODUCTION

Properties of nuclear matter is a basic subject in nuclear physics. The equation of state (EoS) of the symmetric nuclear matter (SNM), which is characterized by the saturation density ρ_0 , the saturation energy $E/A(\rho_0)$ and the incompressibility K_∞ , has been studied for a long time and its properties around ρ_0 are known rather well. In contrast, the EoS of the pure neutron matter (PNM) has not been established, despite its importance connected with compact astrophysical objects, e.g. neutron stars (NSs). Recent observation of a two-solar-mass ($2M_\odot$) NS [1] has imposed a constraint on the EoS, and has given an additional momentum for resolving the PNM EoS in particular. Based on the SNM EoS, the PNM EoS is mostly governed by the symmetry energy S as a function of density ρ , which is characterized by $S_0 = S(\rho = \rho_0)$ and the slope parameter,

$$L = 3\rho_0 \left. \frac{\partial S(\rho)}{\partial \rho} \right|_{\rho=\rho_0}. \quad (1)$$

As S_0 has long been investigated and is known rather well, the current uncertainty in the PNM EoS mainly originates in the uncertainty in L .

Although pure neutron many-body systems do not exist on earth, experiments using radioactive beams disclosed that many nuclei have certain volumes dominated by neutrons; i.e. neutron skins. This may open a possibility to constrain the PNM EoS from experiments on structure of the neutron-rich nuclei. Objects dominated by neutrons may be formed also in the process of nuclear reactions, which could leave a signal in observables. Many studies narrowing the PNM EoS have been devoted to searching observables which strongly correlate with L ; e.g. nuclear mass systematics [2–6], neutron skin thickness [7–12], fragmentation in the heavy ion collisions [13–16], and low-lying $E1$ mode (LED) [17, 18] in

unstable nuclei. Among them, we focus on quantities relevant to structure of specific nuclides, for which model-dependence is considered to be relatively weak.

In Ref. [11], the neutron skin thickness Δr_{np} in ^{208}Pb has been found to correlate linearly to L with a large correlation coefficient 0.98, by calculations using 47 effective interactions. This suggests that accurate determination of Δr_{np} serves constraining L . The LED mode is considered as a relative oscillation between the neutron skin and the remnant core. In Ref. [17], a linear correlation between the LED cross section (σ_{LED}) and L has been suggested, from calculations in the random-phase approximation (RPA) for ^{68}Ni and ^{132}Sn with 26 effective interaction. By combining it with the experimental data, $L = 49 - 81$ MeV has been deduced [19, 20]. However, the covariance analysis for effective interactions [21–23] has shown that this correlation is not always strong. Instead, the dipole polarizability α_D has been claimed to be better in constraining L than cross section and transition strength of the LED. If the α_D - L correlation is assumed, the experimental data in ^{208}Pb indicate $L = 46 \pm 15$ MeV [24]. It has further been argued, in Ref. [25], that a product of α_D and S_0 is better correlated with L than α_D alone, based on the droplet model with some assumptions.

The above four quantities (Δr_{np} , σ_{LED} , α_D and $\alpha_D S_0$) have been proposed in separate works, and there have been few studies comparing them directly, with exception of Ref. [26]. Moreover, depending on the studies, two different types of the correlations have been argued that should be distinguished. The α_D - L correlation has been investigated using the covariance analysis, for which a single interaction and its variants are employed. These variants are generated so as to have similar properties to the original interaction except L . In contrast, the other correlations have been investigated using many interactions with different origin. It is not obvious whether

these two types of correlations have the same behavior. We also point out that nucleus-dependence has not been discussed sufficiently. Most calculations have been implemented in ^{68}Ni , ^{132}Sn and ^{208}Pb , partly because they are spherical, neutron-rich and accessible by experiments. Nuclear deformation possibly draws complication, indeed. Still, there could be better candidates. Further investigation including careful assessment of correlations is desired in order to constrain L from experimental data.

In this article we investigate the correlations of Δr_{np} , σ_{LED} , α_D and $\alpha_D S_0$ with L for a number of spherical nuclei. The paper is organized as follows. In Sec. II, we briefly explain interactions we employ and introduce an additional term to them, which controls the value of L . Numerical results are given in Sec. III, and we discuss the interaction- and nucleus-dependence of the correlations. Conclusion is given in Sec. IV.

II. METHOD

We perform the RPA calculations on top of the Hartree-Fock (HF) wave functions in fully self-consistent manner, by using the numerical methods of Refs. [27, 28].

In investigating interaction-dependence of the correlations between L and the quantities, we employ a variety of effective interactions, covering a wide range of L . They are three Skyrme interactions which have widely been used (SkM* [29], SLy4 [30] and SGII [31]), two latest designed ones (UNEDF0 and UNEDF1 [32]), and four Skyrme interactions (SkI2, SkI3, SkI4 and SkI5 [33]) that give large L values, and two more Skyrme interactions (SkT4 [34] and Ska [35]) which are less frequently used but useful for checking robustness of the correlations. In addition, three Gogny (D1 [36], D1S [37] and D1M [38]) and two M3Y-type interactions (M3Y-P6 and M3Y-P7 [39]) are adopted. Using these effective interactions which cover $L = 18 - 129$ MeV, we discuss the correlations among different interactions (CDI). There have been a certain number of relativistic mean-field (RMF) calculations. Most of the RMF Lagrangians adopted so far tend to give large L values ($\gtrsim 100$ MeV), which do not seem compatible with experimental data. Their results are similar, though not identical, to the SkIn ($n = 2 - 5$) ones. There may be rooms to obtain RMF Lagrangians giving smaller L values. Although we have not implemented the RMF calculations, we shall mention some of the RMF results available in literature.

In the covariance analysis in Refs. [21–23], a class of interactions that share basic properties with an original interaction were considered. Following Ref. [40], we here introduce an additional term for the interaction,

$$v_{ij} \implies v_{ij} - V_L [\rho^\alpha(\mathbf{r}_i) - \rho_0^\alpha] P_\sigma \delta(\mathbf{r}_i - \mathbf{r}_j), \quad (2)$$

where P_σ is the spin exchange operator. This additional term does not change S_0 because it vanishes at $\rho = \rho_0$, and has no effects on the SNM EoS because

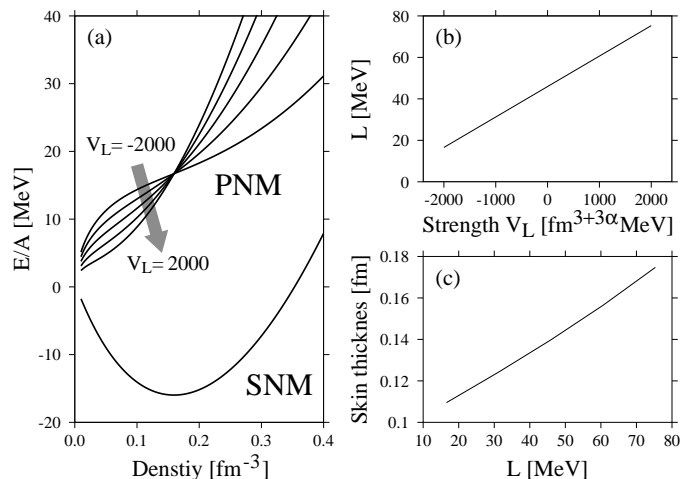


FIG. 1: V_L dependence (Eq. (2)) of (a) EoS and (b) the slope parameter L , calculated with SLy4 interaction on setting $V_L = 0, \pm 1000, \pm 2000$ fm $^{3+3\alpha}$ MeV, and (c) relation between neutron skin thickness in ^{208}Pb and L shifted by adjusting V_L .

$\langle P_\sigma \delta(\mathbf{r}_i - \mathbf{r}_j) \rangle = 0$ in the SNM. We thus obtain a class of interactions having different L by varying V_L , with changing neither SNM EoS nor S_0 . All the non-relativistic interactions contain a density-dependent term in which the coupling constant is proportional to a power of the density. We keep this power α of each original interaction also for the additional term in Eq. (2). The correlation given by the interactions belonging to the same class, which are generated from a single interaction but have different V_L , will be called correlation in a single class of interactions (CSI) in this paper.

Figure 1(a) illustrates how V_L affects the EoS, by taking the SLy4 interaction and its variants with $V_L = 0, \pm 1000, \pm 2000$ fm $^{3+3\alpha}$ MeV as an example. The L value is changed linearly with V_L , as $V_L = -2000$ (2000) fm $^{3+3\alpha}$ MeV shifts L from the original value 46 MeV to 17 (75) MeV. The neutron skin thickness is defined by

$$\Delta r_{np} = \sqrt{\langle r^2 \rangle_n} - \sqrt{\langle r^2 \rangle_p}, \quad (3)$$

for a specific nuclide. As is expected, L correlates linearly with the neutron skin thickness in ^{208}Pb among this class of interactions, as shown in Fig. 1(c). The additional term changes the binding energy of ^{208}Pb by ~ 15 MeV with $V_L = -2000$ (2000) fm $^{3+3\alpha}$ MeV. We do not take this difference seriously, since this energy shift is comparable to the difference of the binding energies obtained from different interactions. For instance, UNEDF0 and UNEDF1 yield 1625 and 1643 MeV for ^{208}Pb , respectively.

The $E1$ transition operator is expressed as

$$\mathcal{O}^{(E1)} = \frac{N}{A} \sum_{i \in p} r_i Y^{(1)}(\Omega_i) - \frac{Z}{A} \sum_{i \in n} r_i Y^{(1)}(\Omega_i), \quad (4)$$

after the center of mass correction. Here i is the index of nucleons and $i \in p$ ($i \in n$) indicates that the sum runs over protons (neutrons). The $E1$ strength is calculated as

$$S^{(E1)}(\omega) = \frac{\gamma}{\pi} \sum_n \left[\frac{1}{(\omega - \omega_n)^2 + \gamma^2} - \frac{1}{(\omega + \omega_n)^2 + \gamma^2} \right] \times \left| \langle \Phi_n | \mathcal{O}^{(E1)} | \Phi_0 \rangle \right|^2 \quad (5)$$

where n is the index of the excited states and ω denotes the excitation energy. For the smearing parameter γ , we adopt $\gamma = 0.5$ MeV, after confirming that the results do not change much with $\gamma = 0.1 - 0.5$ MeV. The LED cross section σ_{LED} is given by

$$\sigma_{\text{LED}} = \frac{16\pi^3 e^2}{9\hbar c} \int_0^{\omega_{\text{dip}}} d\omega \omega S^{(E1)}(\omega), \quad (6)$$

where ω_{dip} is the energy at which $S^{(E1)}(\omega)$ is separated into the LED and giant dipole resonance (GDR) regions. Although the LED and the GDR components could mix in certain energy range [41], we here separate them by energy for simplicity. It is not obvious how ω_{dip} should be defined. We determine ω_{dip} as follows. If we find a distinguishable LED peak in $S^{(E1)}(\omega)$, ω_{dip} is defined as the energy corresponding to the minimum of $S^{(E1)}(\omega)$ that exists between the LED peak and the GDR.

The dipole polarizability α_D is calculated as

$$\alpha_D = \frac{8\pi e^2}{9} \int_0^\infty d\omega \frac{S^{(E1)}(\omega)}{\omega}. \quad (7)$$

Owing to the energy denominator, α_D is expected to be sensitive to the LED. It should be noted that α_D is unambiguously defined unlike σ_{LED} .

As a measure of correlations, it is customary to use the correlation coefficient. For the two quantities (x, y) for which we have data points (x_k, y_k) ($k = 1, 2, \dots, N_d$), the correlation coefficient is given by

$$R[x, y] = \frac{\sum_{k=1}^{N_d} (x_k - \bar{x})(y_k - \bar{y})}{\sqrt{\sum_{k=1}^{N_d} (x_k - \bar{x})^2} \sqrt{\sum_{k=1}^{N_d} (y_k - \bar{y})^2}}, \quad (8)$$

with $\bar{x} = \sum_{k=1}^{N_d} x_k / N_d$ and likewise for \bar{y} . We obtain $|R[x, y]| = 1$ if x and y are fully correlated and $R[x, y] = 0$ if x and y are fully uncorrelated. In the present case k corresponds to individual interaction, covering the interactions mentioned above including the variants with varying V_L . x is fixed to be the slope parameter L , and y is taken to be Δr_{np} , σ_{LED} , α_D or $\alpha_D S_0$ for a specific nuclide.

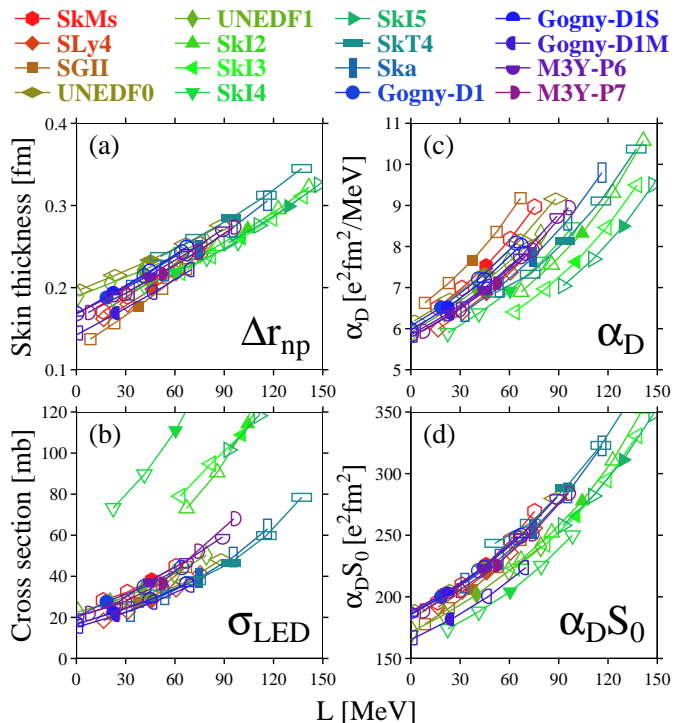


FIG. 2: (Color online) Correlations of the slope parameter L with (a) the neutron skin thickness Δr_{np} , (b) the LED cross section σ_{LED} , (c) the dipole polarizability α_D and (d) $\alpha_D S_0$ of ^{132}Sn . See text for details.

III. NUMERICAL RESULTS

A. Correlations in ^{132}Sn

Figure 2 shows correlations of L with the neutron skin thickness Δr_{np} , the LED cross section σ_{LED} , the dipole polarizability α_D and $\alpha_D S_0$ in ^{132}Sn , obtained by the HF+RPA calculations. Effective interactions are distinguished by colors and symbols, as listed in the upper part of the figure. Results with $V_L = 0$ are represented by full symbols, while those with their $V_L \neq 0$ variants by open symbols. The results of the same class of interactions are connected by lines so as to show the CSIs.

It is seen in Fig. 2(a) that Δr_{np} correlates well with L . Indeed, we obtain $R[L, \Delta r_{np}] = 0.959$. This correlation is well expressed by a linear function, as $\Delta r_{np} = 0.00114L + 0.160$ fm with standard deviation 0.014 fm, by assuming the unit of L to be MeV. With respect to the CSI, the three interactions UNEDF0, UNEDF1 and SkI4 give slopes less than 1.0×10^{-3} fm/MeV, while slopes of the other Skyrme interactions are steeper than 1.2×10^{-3} fm/MeV and those of the Gogny and M3Y interactions fall in the narrow range $(1.15 \pm 0.05) \times 10^{-3}$ fm/MeV. The maximum (minimum) slope is 1.46 (0.83) $\times 10^{-3}$ fm/MeV of SGII (UNEDF1), which deviates by 30% from the value fitting all the interactions (i.e. 1.14×10^{-3} fm/MeV). We note that slopes of the CSI stay

around 1.14×10^{-3} fm/MeV within 10% in more than half of the interactions. The CDI (correlations among the interactions with $V_L = 0$) is strong as well, having $R[L, \Delta r_{np}] = 0.939$. Thus L can be well constrained by Δr_{np} in ^{132}Sn if it is measured precisely. The standard deviation 0.014 fm is converted to an uncertainty of 12 MeV for L .

Correlations between L and σ_{LED} are shown in Fig. 2(b). We discard the σ_{LED} results in the case that $S^{(E1)}(\omega)$ has two peaks in the LED region, because we cannot unambiguously determine ω_{dip} at which the LED and GDR regions are separated, and ω_{dip} may change discontinuously by changing V_L even if we adopt a certain definition. Four interactions SkI2, SkI3, SkI4 and SkI5 and their variants produce quite large σ_{LED} , which clearly deviate from the results of the other interactions. The CSI are not similar even within these four classes of interactions. It is noted that the Gogny and M3Y interactions yield correlations similar to the Skyrme interactions other than the above SkI series. If we ignore the results of the SkI series, $R[L, \sigma_{\text{LED}}] = 0.928$ is obtained and σ_{LED} can be fitted to a linear function of L as $\sigma_{\text{LED}} = 0.399L + 15.4$ mb MeV with the standard deviation 5.0 mb MeV. When we fit σ_{LED} by a quadratic function, we obtain $\sigma_{\text{LED}} = 0.00138L^2 + 0.238L + 18.7$ mb MeV with the standard deviation 4.7 mb MeV. Compared with Ref. [17] (see Fig. 2(b) of Ref. [17]), the slope of the linear function is smaller by a factor ~ 2 . This discrepancy can be interpreted as follows: In Ref. [17], the CDI of σ_{LED} with L has been investigated via 19 Skyrme interactions and 7 relativistic effective Lagrangians which cover $L = 0 - 130$ MeV. Among them, seven relativistic Lagrangians and three Skyrme interactions SkI2, SkI3 and SK255 [42], all of which give $L \gtrsim 100$ MeV, seem to behave differently from the other interactions. The high weight (10 out of the 26 interactions) of these large- L interactions leads to the steep slope in Ref. [17]. If we exclude the results of SkI2, SkI3, SK255 and the RMF in Fig. 2(b) of Ref. [17] and refit the others to a linear function, the slope is compatible with our result. However, with ambiguity in the definition of σ_{LED} and large deviation by certain interactions, we conclude that σ_{LED} is currently unsuitable for constraining L .

Figure 2(c) shows the α_D - L relations. Despite the relatively large value of $R[L, \alpha_D] = 0.90$, the lines representing the CSI are widely scattered. This indicates that the CDI behaves differently from the CSI. If all the results of α_D are fitted to a linear function, we obtain $\alpha_D = 0.0261L + 5.94$ e²fm²/MeV with the standard deviation 0.53 e²fm²/MeV. However, the slopes given by the CSI are significantly larger; 0.031 – 0.051 e²fm²/MeV² with the Skyrme interactions, ~ 0.027 with the Gogny interactions and ~ 0.033 with the M3Y interactions. The intercepts are also distributed in as wide range as 2.14 – 6.15 e²fm²/MeV. It is thus important to take into account the CSI and the CDI simultaneously. The α_D - L correlation might look good when we pay attention only to the CSI like in the previous covariance analysis, and

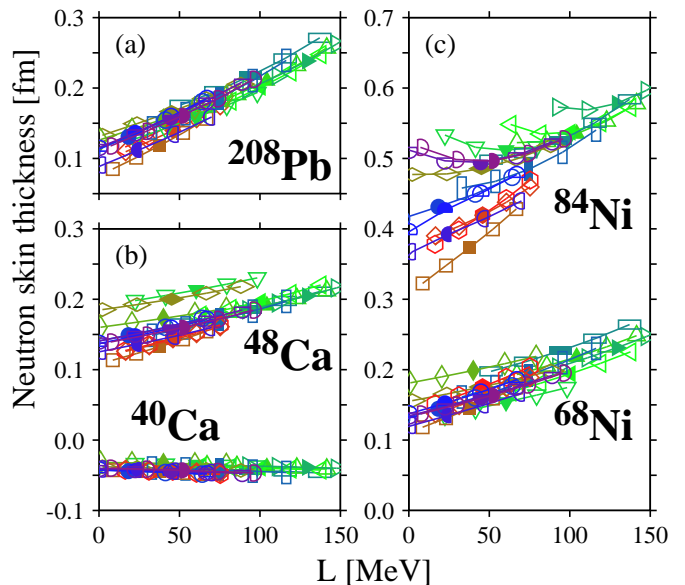


FIG. 3: (Color online) Correlations of Δr_{np} and L in (a) ^{208}Pb , (b) $^{40,48}\text{Ca}$ and (c) $^{68,84}\text{Ni}$. See Fig. 2 for colors and symbols.

likewise to the CDI. However, there exists notable difference between the CSI and the CDI. It is not necessarily suitable to constrain L only by α_D .

The $\alpha_D S_0$ - L correlations are shown in Fig. 2(d). The strong correlation between $\alpha_D S_0$ and L is clearly seen. The correlation coefficient is $R[L, \alpha_D S_0] = 0.953$. The linear fitting gives $\alpha_D S_0 = 1.13L + 170$ e²fm² with the standard deviation 15 e²fm², which corresponds to 13 MeV uncertainty of L , and the quadratic fit gives $\alpha_D S_0 = 0.00393L^2 + 0.617L + 180$ e²fm² with the standard deviation 13 e²fm². Even if we restrict ourselves to the CDI by setting $V_L = 0$, the correlations have similar behavior; $R[L, \alpha_D S_0] = 0.947$, the fitted linear function is $\alpha_D S_0 = 1.08L + 169$ e²fm² with the standard deviation 11 e²fm², and the quadratic function is $\alpha_D S_0 = 0.00208L^2 + 0.773L + 177$ e²fm² with the standard deviation 11 e²fm². As pointed out in Ref. [43], S_0 has positive correlation with L among the interactions with $V_L = 0$. This helps $\alpha_D S_0$ to correlate with L better than α_D alone. Thus $\alpha_D S_0$ will be useful in constraining L , although it requires precise assessment of S_0 .

We have investigated the correlations of Δr_{np} , σ_{LED} , α_D and $\alpha_D S_0$ in ^{132}Sn with L , and have found that Δr_{np} and $\alpha_D S_0$ are promising for constraining L .

B. Nucleus-dependence

The correlations between L and observables related to the neutron skin were discussed mainly in ^{68}Ni , ^{132}Sn and ^{208}Pb in the previous studies. We next consider nucleus-dependence of the Δr_{np} - L and $\alpha_D S_0$ - L correlations.

We have calculated the Δr_{np} - L correlations in doubly-magic nuclei and in nearly-doubly-magic nuclei, $^{16,22,24}\text{O}$, $^{40,48,54,70}\text{Ca}$, $^{68,78,84}\text{Ni}$, $^{132,140,176}\text{Sn}$ and ^{208}Pb , some of which are plotted in Fig. 3. In ^{208}Pb , Δr_{np} correlates well to L , giving $R[L, \Delta r_{np}(^{208}\text{Pb})] = 0.965$. This result is consistent with that reported in Ref. [11]. The linear function obtained by fitting is $\Delta r_{np}(^{208}\text{Pb}) = 0.00107L + 0.103\text{fm}$ with the standard deviation 0.013 fm, being equivalent to 12 MeV uncertainty of L . The slope of the fitted function is smaller by $\sim 30\%$ than that of Ref. [11]. This discrepancy is again attributed to contribution of the RMF results with $L \gtrsim 100\text{MeV}$, because they increase the slope in Fig. 3 of Ref. [11]. Still the Δr_{np} - L correlation in ^{208}Pb is so strong to be promising for getting constraint on L . The Δr_{np} - L correlation gradually becomes the weaker for the lighter nuclei. Notice that the steeper slope in the linear function tends to make the correlation coefficient the larger. When errors in experimental data are taken into consideration, a steep slope is further advantageous in constraining L . As mentioned above, we obtain $R[L, \Delta r_{np}(^{132}\text{Sn})] = 0.959$. In ^{68}Ni , $R[L, \Delta r_{np}(^{68}\text{Ni})] = 0.901$ and the linear fitting gives $\Delta r_{np}(^{68}\text{Ni}) = 0.000761L + 0.133\text{fm}$. In ^{48}Ca , the correlation coefficient drops to $R[L, \Delta r_{np}(^{48}\text{Ca})] = 0.785$ and the linear fitting results in $\Delta r_{np}(^{48}\text{Ca}) = 0.000546L + 0.138\text{fm}$. In the $Z = N$ nuclei ^{16}O and ^{40}Ca , the calculated Δr_{np} 's are almost independent of L . The Δr_{np} - L correlation also becomes weak in drip-line nuclei such as ^{84}Ni , as shown in Fig. 3(c). Δr_{np} is strongly affected by the spatial extension of the loosely-bound neutron orbits around the neutron Fermi level. In nuclei near the neutron drip line, the additional term introduced in Eq. (2) with negative V_L , which lowers L , lifts up the neutron Fermi level and makes the loosely-bound orbits extend significantly. This effect is connected to the neutron halo which may irregularly increase Δr_{np} . This mechanism makes the Δr_{np} - L correlation weaker in neutron drip-line nuclei, as is seen in $^{22,24}\text{O}$, ^{70}Ca and ^{176}Sn .

Therefore, the Δr_{np} in heavy nuclei distant from the drip line may be appropriate in constraining L . Measurement on ^{208}Pb seems to provide one of the best possibilities in this respect. However, despite great efforts and progress, it is not yet easy to experimentally determine $\Delta r_{np}(^{208}\text{Pb})$ with good precision. It should also be kept in mind that the Δr_{np} - L correlation has been investigated only phenomenologically. Without support from quantitatively reliable theories, cross checks from other nuclei and/or other quantities are important.

Let us turn to nucleus-dependence of the $\alpha_D S_0$ - L correlation. Because of the energy denominator in Eq. (7), $\alpha_D S_0$ is rather sensitive to the LED, which emerges and grows up beyond the magic numbers $N = 14, 28, 50$ and 82 [44, 45]. We expect that $\alpha_D S_0$ correlates better with L as the LED develops in the neutron-rich nuclei. In Table I we list $R[L, \alpha_D S_0]$ for the stable doubly-magic nuclei and neutron-rich nuclei having well-developed LED, $^{16,24}\text{O}$, $^{40,48,54}\text{Ca}$, $^{68,84}\text{Ni}$, $^{132,140}\text{Sn}$ and ^{208}Pb . The optimized

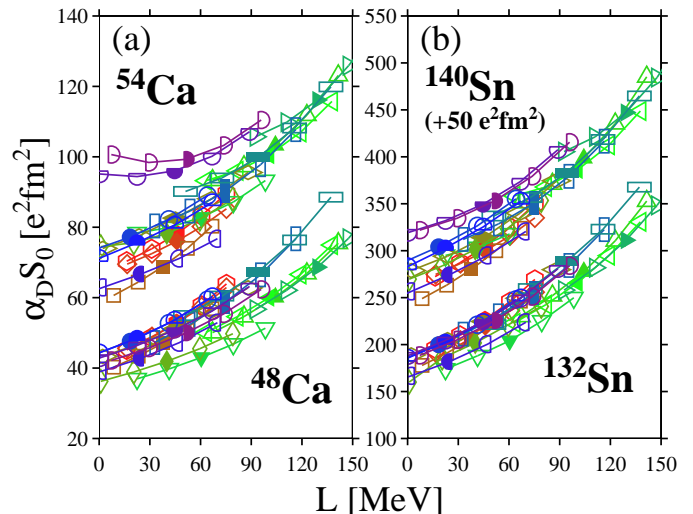


FIG. 4: (Color online) $\alpha_D S_0$ - L correlations in (a) $^{48,54}\text{Ca}$ and (b) $^{132,140}\text{Sn}$. Data of ^{140}Sn is shifted by $50\text{e}^2\text{fm}^2$ to accommodate them with the results of ^{132}Sn in a single plot. See Fig. 2 for colors and symbols.

values of the coefficients a and b when the calculated results are fitted as $\alpha_D S_0 = aL + b$, with the standard deviation σ of the fitting, are shown as well.

The left panel of Fig. 4 illustrates how the LED affects the $\alpha_D S_0$ - L correlation, by comparing the results of ^{54}Ca with those of ^{48}Ca . From ^{48}Ca to ^{54}Ca , $\alpha_D S_0$ becomes larger and the slope of the fitted linear function becomes steeper (0.242 to $0.331\text{e}^2\text{fm}^2/\text{MeV}$). The steep slope is expedient for constraining L from experiment. The LED emergence and development contributes to the $\alpha_D S_0$ - L correlation. However, in ^{54}Ca the $\alpha_D S_0$ - L relation of the M3Y-P6 and P7 interactions deviates significantly from that of the other interactions, while such deviation is not found in ^{48}Ca . As a result, we obtain $R[L, \alpha_D S_0(^{54}\text{Ca})] = 0.86$, smaller than $R[L, \alpha_D S_0(^{48}\text{Ca})] = 0.90$. This is mainly because the M3Y-P6 and P7 interactions produce higher neutron Fermi level than the other interactions in ^{54}Ca , and generate the neutron halo when we take $V_L < 0$. As in Δr_{np} , presence of the halo disturbs the correlation, since the halo may produce large LED and thereby causes large α_D . It can be confirmed experimentally whether or not ^{54}Ca is a halo nucleus. Suppose that the neutron halo is ruled out, ^{54}Ca can be a candidate to constrain L from $\alpha_D S_0$. Excluding the M3Y interactions, we obtain $R[L, \alpha_D S_0(^{54}\text{Ca})] = 0.96$ and steeper slope ($0.40\text{e}^2\text{fm}^2/\text{MeV}$) in the linear fitting. Also for $^{68,84}\text{Ni}$, whereas the slope obtained by the linear fitting becomes steeper in ^{84}Ni , $R[L, \alpha_D S_0(^{84}\text{Ni})] = 0.66$ is small because of the neutron halo. Similar trend is seen in the drip-line nucleus ^{24}O . Before applying $\alpha_D S_0$ in a certain nucleus for constraining L , it should be confirmed that the nucleus does not have halo.

TABLE I: Correlation coefficient $R[L, \alpha_D S_0]$, and the optimized values of the coefficients a and b when the calculated results are fitted as $\alpha_D S_0 = aL + b$, with the standard deviation σ of the fitting.

nucleus ($^A Z$)	$R[L, \alpha_D S_0]$	a [$e^2 \text{fm}^2 / \text{MeV}$]	b [$e^2 \text{fm}^2$]	σ [$e^2 \text{fm}^2$]
^{16}O	0.848	0.068	9.6	1.8
^{24}O	0.628	0.058	9.8	1.5
^{40}Ca	0.881	0.210	33.4	4.7
^{48}Ca	0.898	0.242	39.6	5.0
^{54}Ca	0.857	0.331	69.1	8.4
^{68}Ni	0.929	0.448	70.5	7.6
^{84}Ni	0.662	0.574	142.7	27.7
^{132}Sn	0.953	1.130	170.1	15.2
^{140}Sn	0.934	1.354	213.6	21.9
^{208}Pb	0.927	1.864	336.8	31.8

The correlation coefficients are high both in $^{132,140}\text{Sn}$, $R[L, \alpha_D S_0(^{132}\text{Sn})] = 0.95$ and $R[L, \alpha_D S_0(^{140}\text{Sn})] = 0.93$, as presented in the right panel of Fig. 4. Although $R[L, \alpha_D S_0]$ slightly decreases from ^{132}Sn to ^{140}Sn , the slope becomes steeper. Both nuclei are suitable for constraining L from $\alpha_D S_0$, if α_D is accessible in future experiments.

The $\alpha_D S_0$ - L correlation in ^{208}Pb has been calculated in Ref. [25] employing Skyrme interactions and relativistic Lagrangians, and the linear fitting gives the slope $a = 2.3 e^2 \text{fm}^2 / \text{MeV}$ and the intercept $b = 333 e^2 \text{fm}^2$. Compared with our result, the intercept is almost equal but the slope is steeper. Another result of the $\alpha_D S_0$ - L relation is available from Ref. [46], in which only α_D - L correlation is calculated with a family of relativistic Lagrangian. We can see the $\alpha_D S_0$ - L correlation using those results. The fitted linear function representing the $\alpha_D S_0$ - L correlation of Ref. [46] has the slope $a \sim 2.9 e^2 \text{fm}^2 / \text{MeV}$ and the intercept $b \sim 310 e^2 \text{fm}^2$. The slope is again steeper than our result while the intercept is compatible. Therefore, the currently available RMF results increase the slope but have small impact on the intercept of the $\alpha_D S_0$ - L relation.

C. Comparison with droplet model estimation

The $\alpha_D S_0$ - L correlation has been suggested in Ref. [25] based on the droplet model under some assumptions. The relation of $\alpha_D S_0$ and L reads

$$(\alpha_D S_0)_{\text{DM}} \sim \frac{\pi e^2}{54} A \langle r^2 \rangle \left[1 + \frac{5}{9} \frac{L}{S_0} \frac{\rho_0 - \rho_A}{\rho_0} \right], \quad (9)$$

where $\rho_A \sim 0.1 \text{fm}^{-3}$ [7, 47]. While we have phenomenologically confirmed the $\alpha_D S_0$ - L correlation in preceding sections, it deserves investigating validity of this relation. For a given interaction and a nucleus we evaluate $(\alpha_D S_0)_{\text{DM}}$ from Eq. (9), and compare them to $\alpha_D S_0$ obtained from the HF+RPA calculations.

One of the assumptions in the droplet model is [48, 49]

$$x_A \equiv \frac{9}{4} \frac{S_0}{Q} A^{-1/3} \ll 1, \quad (10)$$

where Q is the surface stiffness coefficient connected with the nuclear surface symmetry energy [2]. For the droplet model estimation (Eq. (9)) to be justified, x_A should be sufficiently small. In evaluating x_A , we use an approximate expression for Q [51],

$$Q \sim \frac{9S_0^2}{8a} \left(\frac{4}{3} \pi \rho_0 \right)^{-1/3} \left(L - \frac{K_{\text{sym}}}{12} \right)^{-1}, \quad (11)$$

instead of calculating Q in the asymmetric semi-infinite nuclear matter [2, 48–50]. Here a ($\sim 0.55 \text{fm}$) is the diffuseness of the symmetric semi-infinite nuclear matter [2] and K_{sym} is the 2nd derivative of the symmetry energy with respect to the density at the saturation point. The calculated x_A values are listed in Table II, accompanying ρ_0 , K_∞ , S_0 , L , K_{sym} and Q .

Figure 5 shows the ratio of $\alpha_D S_0$ calculated with HF+RPA to $(\alpha_D S_0)_{\text{DM}}$ in ^{54}Ca , ^{68}Ni , ^{132}Sn and ^{208}Pb . The ratios clearly deviate from unity even for small x_A . Although we have phenomenologically confirmed the $\alpha_D S_0$ - L correlation, the droplet model is not necessarily appropriate for justifying the correlation.

IV. CONCLUSION

We have investigated the correlations of L with the following four quantities; the neutron skin thickness Δr_{np} , the cross section of the low-energy dipole (LED) mode σ_{LED} , the dipole polarizability α_D , and the product of α_D and the symmetry energy S_0 . In order to directly compare them and to unravel disorder in observables constraining L , we have simultaneously discussed the correlations derived from different interactions (CDI) and the correlation in a single class of interactions (CSI). For the

TABLE II: Saturation density ρ_0 , incompressibility of symmetry nuclear matter K_∞ , symmetry energy S_0 , slope parameter L , incompressibility of symmetry energy K_{sym} , surface stiffness parameter Q and x_A multiplied by the mass dependence, given by the Skyrme, Gogny and M3Y interactions with $V_L = 0$.

	ρ_0 [fm $^{-3}$]	K_∞ [MeV]	S_0 [MeV]	L [MeV]	K_{sym} [MeV]	Q [MeV]	$x_A \times A^{1/3}$
SkM*	0.160	216.4	30.0	45.8	-155.8	35.9	1.88
SLy4	0.160	229.9	32.0	45.9	-119.7	42.8	1.68
SGII	0.158	214.5	26.8	37.7	-145.8	33.9	1.78
UNEDF0	0.160	229.8	30.5	45.1	-189.6	35.8	1.92
UNEDF1	0.159	219.8	29.0	40.0	-179.4	35.8	1.82
SkI2	0.157	240.7	33.4	104.3	70.6	26.6	2.82
SkI3	0.158	258.0	34.8	100.5	72.9	30.2	2.60
SkI4	0.160	247.7	29.5	60.4	-40.6	31.9	2.08
SkI5	0.156	255.6	36.6	129.3	159.4	27.3	3.02
SkT4	0.159	262.9	35.5	94.1	-24.5	30.6	2.60
Ska	0.155	235.3	32.9	74.6	-78.4	31.5	2.35
D1	0.166	229.4	30.7	18.4	-274.6	41.4	1.67
D1S	0.163	202.9	31.1	22.4	-241.5	41.0	1.71
D1M	0.165	225.0	28.6	24.8	-133.2	41.0	1.57
M3Y-P6	0.163	239.7	32.1	44.6	-165.3	31.8	2.27
M3Y-P7	0.163	254.7	31.7	51.5	-127.8	29.2	2.45

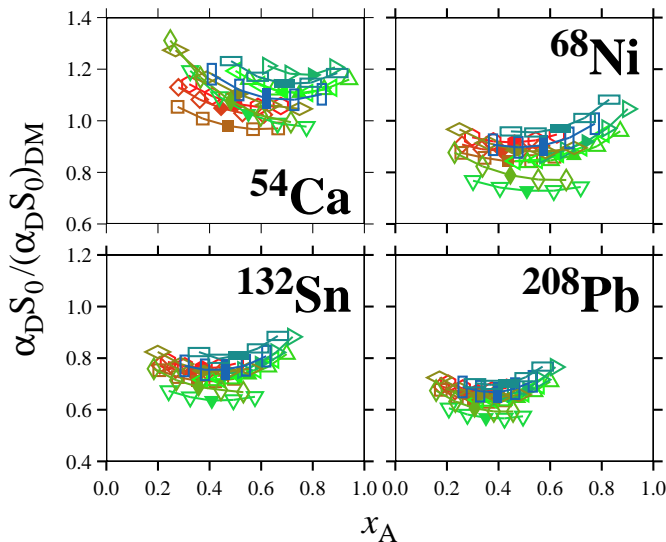


FIG. 5: (Color online) Ratio of $\alpha_D S_0$ obtained from the HF+RPA calculations to the droplet model estimate in ^{54}Ca , ^{68}Ni , ^{132}Sn and ^{208}Pb . See Fig. 2 for colors and symbols.

latter we introduce an additional term to each interaction, which enables us to control the value of L without influencing SNM EoS and S_0 .

The Δr_{np} correlates almost linearly with L in heavy nuclei, although there remains slight interaction-dependence as recognized via comparison with the results in Ref. [11]. The $\sigma_{\text{LED}}-L$ correlation has a signifi-

cant interaction-dependence. Together with ambiguity in its definition, σ_{LED} is not recommended to constraining L . In the α_D-L correlation, we have found that the CSI and the CDI behave differently. It is not reasonable to constrain L only from α_D . The $\alpha_D S_0-L$ correlation works well for narrowing down L . The Δr_{np} and $\alpha_D S_0$ are promising for constraining L , though with ~ 12 MeV uncertainty.

The nucleus-dependence of the $\Delta r_{np}-L$ and $\alpha_D S_0-L$ correlations has also been discussed. While the neutron halo makes the correlations weak, these correlations are strong in neutron-rich medium- or heavy-mass nuclei without neutron halo. Except neutron-halo nuclei, the LED makes the $\alpha_D S_0-L$ correlation strong and the slope of the linear function steep, to which the HF+RPA results are well fitted. Consequently, the neutron-rich nuclei having well-developed LED (e.g. ^{54}Ca and ^{140}Sn) are good candidates for obtaining the constraint on L , as well as the doubly magic nuclei ^{132}Sn and ^{208}Pb .

Acknowledgments

We thank K. Iida for fruitful discussions. This work is financially supported as Grant-in-Aid for Scientific Research on Innovative Areas, No. 24105008, by The Ministry of Education, Culture, Sports, Science and Technology, Japan. A part of numerical calculations were performed on HITAC SR16000s at IMIT in Chiba University, ITC in University of Tokyo, IIC in Hokkaido University, and YITP in Kyoto University.

-
- [1] P.B. Demorest, T. Pennucci, S.M. Ransom, M.S.E. Roberts, and J.W.T. Hessels, *Nature* **467**, 1081-1083 (2010).
- [2] P. Danielewicz and J. Lee, *Nucl. Phys. A* **818** (2009) 36-96.
- [3] M. Kortelainen, T. Lesinski, J. Moré, W. Nazarewicz, J. Sarich, N. Schunck, M.V. Stoitsov, and S. Wild, *Phys. Rev. C* **82**, 024313 (2010).
- [4] M. Liu, N. Wang, Z.-X. Li, and F.-S. Zhang, *Phys. Rev. C* **82**, 064306 (2010).
- [5] J. Dong, W. Zuo, J. Gu, and U. Lombardo, *Phys. Rev. C* **85**, 034308 (2012).
- [6] P. Möller, W.D. Myers, H. Sagawa, and S. Yashida *Phys. Rev. Lett.* **108**, 052501 (2012).
- [7] M. Centelles, X. Roca-Maza, X. Viñas, and M. Warda, *Phys. Rev. Lett.* **102**, 122502 (2009).
- [8] M. Warda, X. Viñas, X. Roca-Maza, and M. Centelles *Phys. Rev. C* **80**, 024316 (2009).
- [9] L.-W. Chen, C.M. Ko, B.-A. Li, and J. Xu, *Phys. Rev. C* **82**, 024321 (2010).
- [10] J. Zenihro *et al.*, *Phys. Rev. C* **82**, 0244611 (2010).
- [11] X. Roca-Maza, M. Centelles, X. Viñas, and W. Warda, *Phys. Rev. Lett.* **106**, 252501 (2011).
- [12] B.K. Agrawal, J.N. De, and S.K. Samaddar, *Phys. Rev. Lett.* **109**, 262501 (2012).
- [13] L.-W. Chen, C.M. Ko, and B.-A. Li *Phys. Rev. Lett.* **94**, 032701 (2005).
- [14] M.A. Famiano *et al.*, *Phys. Rev. Lett.* **97**, 052701 (2006).
- [15] D.V. Shetty, S.J. Yennello, and G.A. Souliotis, *Phys. Rev. C* **76**, 024606 (2007).
- [16] M.B. Tsang *et al.*, *Phys. Rev. Lett.* **102**, 122701 (2009).
- [17] A. Carbone, G. Colò, A. Bracco, L.-G. Cao, P.F. Bortignon, F. Camera, and O. Wieland, *Phys. Rev. C* **81**, 041301(R) (2010).
- [18] T. Inakura, T. Nakatsukasa, and K. Yabana, *Phys. Rev. C* **88**, 051305(R) (2013).
- [19] O. Wieland *et al.*, *Phys. Rev. Lett.* **102**, 092502 (2009).
- [20] P. Adrich *et al.*, *Phys. Rev. Lett.* **95**, 132501 (2005).
- [21] N. Paar, A. Horvat, *EPJ Web of Conferences* **66**, 02078 (2014)
- [22] P.-G. Reinhard and W. Nazarewicz, *Phys. Rev. C* **81**, 051303 (2010).
- [23] X. Roca-Maza, N. Paar, and G. Colò, arXiv:1406.1885.
- [24] A. Tamii *et al.*, *Phys. Rev. Lett.* **107**, 062502 (2011).
- [25] X. Roca-Maza, M. Brenna, G. Colò, M. Centelles, X. Viñas, B.K. Agrawal, D. Vretenar, and J. Piekarewicz, *Phys. Rev. C* **88**, 024316 (2013).
- [26] P.-G. Reinhard, J. Piekarewicz, W. Nazarewicz, B.K. Agrawal, N. Paar, and X. Roca-Maza, *Phys. Rev. C* **88**, 034325 (2013).
- [27] T. Inakura, T. Nakatsukasa, and K. Yabana, *Phys. Rev. C* **80**, 044301 (2009).
- [28] H. Nakada, K. Mizuyama, M. Yamagami, and M. Matsuo, *Nucl. Phys. A* **828**, 283 (2009).
- [29] J. Bartel, P. Quentin, M. Brack, C. Guet, and H.B. Håkansson, *Nucl. Phys. A* **386** (1982) 79.
- [30] E. Chabanat, P. Bonche, P. Heenen, J. Meyer, and R. Schaeffer, *Nucl. Phys. A* **635**, 231 (1998).
- [31] N.V. Giai, and H. Sagawa, *Phys. Lett.* **B 106**, 379 (1981).
- [32] M. Kortelainen, J. McDonnell, W. Nazarewicz, P.-G. Reinhard, J. Sarich, N. Schunck, M.V. Stoitsov, and S.M. Wild, *Phys. Rev. C* **85**, 024304 (2012)
- [33] P.-G. Reinhard and H. Flocard, *Nucl. Phys. A* **584**, (1995) 467.
- [34] F. Tondeur, M. Brack, M. Farine, and J.M. Pearson, *Nucl. Phys. A* **420** (1984) 297.
- [35] H.S. Kohler, *Nucl. Phys. A* **258** (1976) 301.
- [36] J. Dechargé and D. Gogny, *Phys. Rev. C* **21**, 1568 (1980).
- [37] J. F. Berger, M. Girod, and D. Gogny, *Nucl. Phys. A* **428**, 23c (1984).
- [38] S. Goriely, S. Hilaire, M. Girod, and S. Péru, *Phys. Rev. Lett.* **102**, 242501 (2009).
- [39] H. Nakada, *Phys. Rev. C* **87**, 014336 (2013).
- [40] A. Ono, P. Danielewicz, W.A. Friedman, W.G. Lynch, and M.B. Tsang, *Phys. Rev. C* **68**, 051601(R) (2003).
- [41] H. Nakada, T. Inakura, H. Sawai, *Phys. Rev. C* **87**, 034302 (2013).
- [42] B.K. Agrawal, S. Shlomo, and V. Kim Au, *Phys. Rev. C* **68**, 031304 (2003).
- [43] J.M. Lattimer and Y. Lim, *Astrophys. Jour.* **771**, 51 (2013).
- [44] T. Inakura, T. Nakatsukasa, and K. Yabana, *Phys. Rev. C* **84**, 021302(R) (2011).
- [45] S. Ebata, T. Nakatsukasa, and T. Inakura, *Phys. Rev. C* **90**, 024303 (2014).
- [46] D. Vretenar, Y.F. Niu, N. Paar, and J. Meng, *Phys. Rev. C* **85**, 044317 (2012).
- [47] N. Wang, M. Liu, H. Jiang, J.L. Tian, and Y.M. Zhao, *Phys. Rev. C* **91**, 031304 (2015).
- [48] W.D. Myers and W.J. Swiatecki, *Ann. Phys.* **55**, 395 (1969).
- [49] M. Brack, C. Guet, and H.-B. Håkansson, *Phys. Rep.* **123**, 275 (1985)
- [50] M. centelles, M.D. Estal, and X. Viñas, *Nucl. Phys. A* **635**, 193 (1998).
- [51] L.-W. Chen, *Phys. Rev. C* **83**, 044308 (2011).